

# Craniometric differentiation suggests disruptive selection on body size among sympatric brocket deer

Andre De Lima<sup>1</sup>, María Martha Torres Martínez<sup>1,2</sup>, José Maurício Barbanti Duarte<sup>3</sup>, Susana González<sup>4,5</sup>

<sup>1</sup>Capão da Imbuia Natural History Museum (MHNCI)

<sup>2</sup>Universidade Federal da Integração Latino-Americana (UNILA)

<sup>3</sup>Universidade Estadual Paulista Júlio de Mesquita Filho

<sup>4</sup>Instituto de Investigaciones Biológicas Clemente Estable

<sup>5</sup>Deer Specialist Group, IUCN Species Survival Commission

María Martha Torres Martínez -  [0000-0002-5892-0788](#)

José Maurício Barbanti Duarte -  [0000-0002-7805-0265](#)

Susana González -  [0000-0001-6470-6182](#)

## Abstract:

The value of craniometrics in classifying brocket deer has been a topic of debate, with its effectiveness within this genus being unclear. This study addressed this uncertainty by examining craniometric data from sympatric species of brocket deer. We present a dataset integrating both published and original data, to elucidate the potential species differentiation by analyzing the inter- and intraspecific variation. Leave-one-out cross-validation (LOOCV) yielded >95% accuracy in species classification. We observed that variation in skull size primarily involves overall size changes rather than specific variation in skull shape among the species. Our findings demonstrate the effectiveness of multivariate craniometric data for taxonomic classifications and offer valuable insights into the evolutionary dynamics of brocket deer species. The observed multidimensional distinction among brocket deer skulls suggests that disruptive selection plays a key role in driving differences in body size across species, while latitude might be an additional important confound factor.

**Keywords:** ecology, taxonomy, evolution, Mazama, brocket deer, craniometrics.

**Received:** 2024-06-28

**Revised:** 2024-11-13

**Accepted:** 2024-11-15

**Final review:** 2024-09-09

## Short title

Craniometric differentiation among sympatric brocket deer

## Corresponding author

Andre De Lima

Capão da Imbuia Natural History Museum (MHNCI); email: andremxlima@gmail.com

## Introduction

Neotropical brocket deer are a group of cryptic species that inhabit tropical and subtropical forests (Gallina-Tessaro et al., 2019; González et al., 2018). The taxonomic status of the group has been updated primarily through karyotype and DNA analysis, revealing that brocket deer are, in fact, a polyphyletic group, with members from three main subtribal clades (Sandoval et al., 2024; Morales-Donoso, 2023; Bernegossi et al., 2023; Peres et al., 2021a; Mantellatto et al., 2022; Heckeberg, 2020; Mantellatto et al., 2020). *Mazama* Rafinesque, 1817 remains the most diverse genus among brocket deer, with species belonging to the *Odocoileina* subtribe (Sandoval et al., 2024). Despite these advances, most of these species are classified in threatened categories, with six species of *Mazama* listed as vulnerable by the IUCN (IUCN 2024; e.g., Vogliotti et al., 2016; Duarte et al., 2015). However, the data are often outdated due to new taxonomic classifications or insufficient information for accurate categorisations (e.g., *Mazama rufa*, Peres et al., 2021a).

One major issue in improving the understanding of species occurrence, and therefore updating conservation strategies, is the challenge of identifying brocket deer species based on morphological traits, even when voucher specimens are available (Peres et al., 2021b). The lack of more detailed information on voucher specimens has hindered the study of the tribe *Odocoileini* (Gutiérrez et al., 2017), emphasizing the need for more reliable identification methods. Improving accuracy in species identification among this group is crucial, especially for sympatric species. In particular, in a large portion of non-Amazon South America, five brocket deer species have partially overlapped geographic distributions, mainly at the tropical/subtropical regional transition in southern Brazil (Oliveira et al., 2022, Peres et al., 2021a). These species include four *Mazama* species (*M. rufa*, *M. americana*, *M. jucunda*, and *M. nana*) and the revalidated *Subulo gouazoubira*, a member of the subtribe *Blastocerina* (Sandoval et al., 2023; Bernegossi et al., 2023; Heckeberg, 2020).

Classification based on external morphological traits is suitable for some paired comparisons but often requires skin preservation and body measurements (Gippoliti and Aloise, 2016). Characteristics of body size and hair colour, position, and morphology have been tested for discriminating between deer species locally and globally; however, several limitations are known (Hua et al., 2020; Silva et al., 2020). Previous attempts to group brocket deer species particularly based on craniometrics have yielded inconclusive results (Merino et al., 2005; Rossi, 2000). Also, several morphological-based identifications of voucher specimens in natural history museum collections have been revised following molecular analysis (Mantellatto et al., 2020). This indicates that previous morphological identifications likely included misclassified specimens, impacting taxonomy and conservation planning (Peres et al., 2021b). Given that genetic approaches remain costly, time-consuming, and not always feasible (e.g., due to the lack of properly preserved tissue samples), there is a need for accessible and reliable taxonomic methods to classify brocket deer specimens (Pires and Marinoni, 2010).

More recently, factorial and principal component analyses have shown some success in differentiating *Mazama* species based on craniometrics (González et al., 2018; Peres et al., 2021a), suggesting that multivariate approaches can be effective for species distinction and for exploring the importance of variation in skull traits (Croitor, 2024; Machado and Teta, 2020). However, besides the historical bias from misidentifications (Mantellatto et al., 2020), small sample sizes have been a general issue in previous comparative analyses. Improving the sample size of correctly identified specimens could provide better insights into the potential

66 for distinguishing sympatric brocket deer through predictive multivariate analysis of  
67 craniometrics. In an applied context, skulls are often the most available voucher material in  
68 museums, mostly from road-killed specimens (Gippoliti and Aloise, 2016). Thus,  
69 understanding how to classify brocket deer species based on craniometrics would  
70 significantly enhance the accuracy of identifying voucher specimens in natural history  
71 collections.

72 Unravelling potential patterns of species differentiation through craniometrics is also  
73 ecologically important for understanding whether these partially sympatric species have  
74 undergone distinct evolutionary processes that might explain differences in skull traits  
75 (Munkhzul et al., 2018; Mahmoudi et al., 2017). At a macroecological scale, many mammal  
76 species, including cervids, show size variations consistent with Bergmann's rule, which links  
77 latitudinal variation to body size due to thermoregulatory needs (Clauss et al., 2013; McNab,  
78 2010; Diniz-Filho et al., 2007; Ashton, 2004; Ashton et al., 2000), though findings have been  
79 inconsistent for cervids (Gohli and Voje, 2016). The lack of robust evaluations of intra- and  
80 interspecific variation in skull size and shape among brocket deer makes this study critical for  
81 understanding the evolutionary forces driving speciation and natural selection within this  
82 group (González et al., 2018).

83 Here, we pooled available published data on craniometry of non-Amazon *Mazama* and  
84 *Subulo* species with a new dataset of individuals identified primarily through genetic analysis  
85 and distinct skin traits. We tested whether linear discriminant functions can effectively  
86 classify species based on craniometrics and whether skull size and shape vary among species.  
87 Additionally, we examined whether a latitudinal evolutionary trend (Tamagnini et al., 2021)  
88 could be observed for a widely distributed species, *S. gouazoubira*. This broader  
89 understanding of intraspecific skull variation is important for improving the accuracy of  
90 species classification at a regional level and may provide insights into the evolutionary  
91 history of brocket deer.

## 92 **Material and methods**

### 93 *Data source*

94 We gathered craniometric data from a total of 80 skulls representing five brocket deer species  
95 from six distinctive sources, including published studies and original datasets (Table 1).  
96 Literature sources included Sandoval et al., (2023), Bernegossi et al., (2023), Peres et al.,  
97 (2021a), González et al., (2018), and Borges (2017). Species identifications from González et  
98 al., (2018) were updated according to Mantellatto et al., (2020). Additionally, original data  
99 were gathered from specimens housed at the Natural History Museum of Curitiba (MHNCI)  
100 in Paraná State, Brazil, based on molecular identifications provided by Mantellatto et al.,  
101 (2020) (n=26), supplemented by additional identifications based on morphological traits  
102 (n=11). We excluded infants and young juveniles and included subadults as well as adults in  
103 the sample data, based on the presence of the third molar and/or antler development. The  
104 inclusion of subadults aimed to capture the intraspecific variability present in natural museum  
105 collections and to increase the effective sample size.

### 106 *Craniometrics*

We measured 35 skull dimensions using a digital calliper (accuracy: 0.1mm), following the criteria outlined by Von den Driesch (1976). The measured traits included total length (LT), condylobasal length (CBL), basal length (BL), short skull length (SSL), premolar 1 – prosthion (PREPRO), basicranial axis (BACR), basifacial axis (BAF), median frontal length (MFL), lambda-nasion (LN), lambda-rhinion (LR), lambda-prosthion (LP), akrokranium (ACI), greatest length of the nasals (GLN), median palatal length (MPL), oral palatal length (OPL), lateral length of the premaxilla (LLPRMAX), length of the cheektooth row (LCHEE), length of the molar row (LMR), length of the premolar row (LPREM), greatest inner length of the orbit (GLOR), greatest inner height of the orbit (GHOR), greatest mastoid breadth (GMBOO), greatest breadth of the occipital condyles (GBOC), greatest breadth at the bases of the paraoccipital processes (GBPP), greatest breadth of the foramen magnum (GBFM), height of the foramen magnum (HFM), greatest neurocranium breadth (GBBC), least frontal breadth (LFBO), greatest breadth across the orbits (GBAO), least breadth between the orbits (LBBO), zygomatic breadth (ZYB), greatest breadth across the nasals (GBN), greatest breadth across the premaxillae (GBPM), and basion (defined as the highest point of the superior nuchal crest – BNUCR).

### Statistical analyses

All statistical analyses were conducted using R version 4.4.1 (R Core Team, 2024). Missing data, accounting for 8.8% of the entire dataset, were handled through imputation rather than the exclusion of observations or variables, following the methodology outlined by Mera-Gaona et al., (2021). Data imputation was performed using the multivariate imputation by chained equations (MICE) package, employing the predictive mean matching method (Van Buuren and Groothuis-Oudshoorn, 2011), with a fixed seed value of 1.

We included *M. rufa* (n=4) within *M. americana* (referred to as the *americana* group) in the analyses due to both the low sample size and the historical uncertainty surrounding the classification of *M. rufa* specimens as *M. americana* before its recent taxonomic revision (Peres et al., 2021a). Age was treated as a binary variable, distinguishing between the subadult (0) and adult (1) classes. We were unable to include sex classes in the analysis due to sample size limitation.

Prior to analysis, multivariate normality of the data was assessed using the Henze-Zirkler and Mardia tests, implemented in the "MVN" package (Korkmaz et al., 2014). Data were log-transformed, and multivariate normality was confirmed through both Henze-Zirkler (HZ = 0.99,  $p > 0.05$ ) and Mardia tests (Skewness = 7907.56,  $p > 0.05$ , Kurtosis = -0.95,  $p > 0.05$ ; Suppl. Fig. 1). Multicollinearity was evaluated by pairwise correlations tests using the function "cor" from the default package "stats", and by estimating variance inflation factor (VIF), using the function "vif" from the "car" package (Fox and Weisberg, 2019).

Linear discriminant function analysis (LDA) was performed using the "lda" function from the "MASS" package (Venables and Ripley, 2002) to assess the potential for discriminating among groups based on craniometric variables. To evaluate the effects of multicollinearity on classification results, we compared the accuracy of the confusion matrix from the LDA with that of a correlation-adjusted Shrinkage Discriminant Analysis (SDA), using the "sda" package (Ahdesmaki et al., 2021). We used Pillai, Wilks, Hotelling-Lawley, and Roy's tests, implemented via the "manova" function, to evaluate differences among group scores. The percentage of explained variance was obtained for each discriminant function and individual variable. Grouping patterns were visually analyzed using observation scores, depicted in up to three-dimensional plots generated using the "plotly" package (Sievert, 2020).

Model validation was conducted through cross-validation techniques (James et al., 2013), including leave-one-out (LOOCV) and K-fold cross-validation (with fold sizes of K = 5, 10, and 15), allowing comparisons of model performance. Average success rate and F-score were employed to assess model performance. F-score provides a balanced measure of the model's accuracy by combining precision and recall into a single value. We set recall and precision as evenly weighted – the F1-score (see Li et al., 2016).

Two approaches were used for evaluating the full model reduction. First, we reran the analysis using only the ten most important variables for each axis and compared the results with the full model. Second, we applied a stepwise forward variable selection method based on Wilk's Lambda criterion using the 'greedy.wilks' function from the 'klaR' package (Weihs et al., 2005). Variables were included at a significance level of  $p=0.05$ . The selected variables were then used to run discriminant analysis on a simplified dataset for comparison with the full model. Additionally, pairwise t-tests were conducted to explore differences among groups in univariate analysis.

To investigate the influence of latitude on the craniometrics of *S. gouazoubira*, linear regression was performed using the most important skull variables as dependent variables, with latitude as the continuous independent variable. The most important variables were determined based on their contribution to the full model, stepwise selection, and univariate analysis, specifically those variables that significantly distinguished *S. gouazoubira* from the other species.

## Results

### *Linear discriminant analysis*

Correlation exceeded 0.5 in 68% of the pairwise comparisons between variables, and VIF values were above 10 for 18 (~50%) of the variables (LT, CBL, BL, SSL, PREPRO, BACR, BAF, MFL, LN, LR, LP, ACI, GLN, OPL, LCHEE, GBOC, GBAO, ZYB). To assess the impact of multicollinearity on classification, we compared the accuracy between LDA and SDA. The LDA of the full model correctly classified 97.5% of brocket deer species observations (Table 2), while the classification accuracy applying SDA was 96.3%. Therefore, we proceeded with LDA results for further analysis. MANOVA tests indicated significant differences for the overall LDA (Pillai = 2.09,  $p < 0.05$ ; Wilks = 0.01,  $p < 0.05$ ; Hotelling-Lawley = 11.96,  $p < 0.05$ ; Roy = 8.79,  $p < 0.05$ ) as well as for each component (LD1:  $F = 228.35$ ,  $p < 0.05$ ; LD2:  $F = 66.15$ ,  $p < 0.05$ ; LD3:  $F = 24.97$ ,  $p < 0.05$ ).

The first discriminant axis (LD1) had the highest eigenvalue (180.27), explaining 76.3% of the total variance. LD2 had an eigenvalue of 38.44 (15.4% of the variance), and LD3 had an eigenvalue of 27.6 (8.3% of the variance). Coefficient scores for each variable and discriminant function are shown in Suppl. Table 1. The distribution of individual scores for LD1 showed significant group segregation, with some overlap in boundary areas (Fig. 1). The ten most important morphological traits for classification along LD1 accounted for 85% of its variance, with 32% solely explained by SSL. For LD2 and LD3, BL contributed 11% to LD2, while LR accounted for 26% of LD3. Nine variables ranked among the top ten contributors to two axes: BAF, BL, GBBC, GHOR, LCHEE, LN, LP, LR, and MFL (Table 3).

Plotting the first and second axes, which together explained 91.7% of the variance, highlighted the distinct influences of each variable on species classification (Fig. 2). SSL and LP were key for distinguishing species of the *americana* group, while LR, LT, and MFL

differentiated *M. jucunda* and *S. gouazoubira*. BL, LR, and GBBC were the most influential traits in separating *M. nana* from the others. A 3D scatterplot of individual coefficients across all discriminant functions showed clear separation among the four groups, with minimal overlap at the boundaries (Fig. 3; see Suppl. Mat. 2 for an interactive plot).

#### *Cross-validation of full model*

Cross-validation using the LOOCV method correctly classified 96.1% of the observations among the four groups/species. The average F1-score for the three configurations of the K-fold method ranged between 0.87–0.90, while the total variance from tests among all K-fold combinations ranged from 60–100% of correct classifications (Fig. 4).

#### *Model simplification*

##### *1) LDA-basis simplified model*

The discriminant analysis with the 20 variables representing the 10 most relatively important for each axis in the full model (Table 3) plus AGE\_dummy resulted in differences among groups (Pillai = 1.87,  $p < 0.05$ ; Wilks = 0.03,  $p < 0.05$ ; Hotelling-Lawley = 9.71,  $p < 0.05$ , Roy = 7.75,  $p < 0.05$ ). The first axis explained 81% of the total variance, with SSL remaining the most important trait (Suppl. Table 2), while the subsequent axes explained 10% and 9%, respectively. The overall F1-score for the classifications by group was 0.94, with 100% of correct classifications for the *americana* group, 90.3% for *M. jucunda*, 93.3% for *S. gouazoubira*, and 86.9% for *M. nana*. Cross-validation by LOOCV resulted in greater F1-score (0.90) than by K-fold (0.80–0.83).

##### *2) Stepwise selection-basis simplified model*

Stepwise forward selection indicated nine morphological traits as important variables, with LP as the most important trait (Suppl. Table 3). The discriminant analysis with these variables resulted in differences among groups (Pillai = 1.73,  $p < 0.05$ ; Wilks = 0.04,  $p < 0.05$ ; Hotelling-Lawley = 7.12,  $p < 0.05$ , Roy = 5.61,  $p < 0.05$ ). The first axis explained 81.4% of the total variance, with ZYB as the most important trait (Suppl. Table 4), while the subsequent axes explained 11.3% and 7.2%, respectively. The F1-score for the classifications by group was 0.94, with 100% for the *americana* group, 89.6% for *M. jucunda*, 93.5% for *S. gouazoubira*, and 86.9% for *M. nana*. Cross-validation by LOOCV resulted in greater F1-score (0.91) than by K-fold (0.78–0.81).

#### *Univariate analysis*

Results of univariate pairwise t-tests with the log-transformed data were significant in 79% of 210 paired tests. Simultaneously distinguishing the four groups occurred with eight variables (LT, LP, CBL, BL, BAF, LLPRMAX, LCHEE, MFL). Tests with significant results distinguishing at least three groups occurred as follows: 13 variables distinguished the groups *americana* and *M. jucunda* from the others (ZYB, OPL, SSL, LR, ACI, GLOR, GBPP, GBAO, GLN, GBBC, LMR, LFBO, LN), three variables distinguished *M. americana* and *M. nana* from the others (BNUCR, PREPRO, MPL), while only one distinguished *S. gouazoubira* and *M. nana* simultaneously (LPREM) (Suppl. Table 5).

### Latitudinal variance in *S. gouazoubira*

A total of 12 variables among those considered the most important were tested as dependent variables of latitude in the linear regression models. Nine of them had significant results, with BAF having the greatest influence ( $R^2 = 0.53$ , Table 4, Fig 5).

## Discussion

The application of linear discriminant function analysis to assign brocket deer species based on their craniometrics yielded a significant success rate, particularly when considering the full model including the standard 35 skull variables (along with age). Although the use of reduced models resulted in a slight decrease in the success rate of classifications, the outcomes remained relatively similar. This suggests that further strengthening of model simplification could be achieved with a larger sample size per group (Maas and Hox, 2005). Thus, our study demonstrates that using observations of confirmed identified individuals leads to high accuracy in classification modelling by linear discrimination functions (Thier et al., 2020). Therefore, there is substantial potential for applying linear discriminant functions to successfully classify unidentified specimens of mammals (Suchentrunk et al., 2007), including brocket deer (González et al., 2018). Furthermore, our findings highlight the importance of predictive multivariate analysis with craniometrics as an additional tool for supporting taxonomic distinctiveness among brocket deer species.

In overview, *Mazama americana* can be distinguished from other species due to their greater size in most skull traits, while the opposite is true for *M. nana* (Peres et al., 2021a; Abril et al., 2010). The inclusion of *M. jucunda* in the comparisons results in three well-distinct size classes, even when considering only the first discriminant dimension. However, the addition of *S. gouazoubira* in the comparisons introduces some overlap in the distribution of observations of skull traits (Fig. 1). These patterns place the latter species between *M. jucunda* and *M. nana*, which become clearly evident only when considering the three dimensions of discriminant analysis (Fig. 2 and 3). Although some variables were able to distinguish the four species classes in the univariate approach, overlapping confidence intervals were frequent due to the small scale of the variables, making univariate comparisons unreliable for species identification (Suppl. Table 5). However, when significant, univariate tests consistently showed the same body size order that we found in the multivariate analysis, suggesting an overall allometric differentiation trend among the species. These results support previous study that did not find differences in skull shape patterns in three-dimensional comparisons among some *Mazama* and *S. gouazoubira*, which all have similar short-nosed skulls compared to larger species (Merino et al., 2005).

### Relative Influence of Skull Traits

Nearly one-third of the skull variables were highlighted by the discriminant functions, with almost half of the total variance in the full model explained by SSL and LR sizes, which are highly correlated ( $r=0.79$ ) and dominated the first and third axes. SSL represents the size between the first pair of premolars and the basion of the cranium, while LR adds the distance between premolars and the rhinion to the measurement (Von den Driesch, 1976). However, among other important variables, width-related ones such as ZYB, GBBC, and GBOC, along with variables representing specific traits like the orbital area (GHOR and GLOR), also showed significant relative influence. Thus, the most important skull variables were related to

284 general three-dimensional allometric differences, not solely the length of the skull. Although  
285 length-related variables were key for explaining the observed variance in multivariate  
286 analysis and distinguishing the four groups/species, their scale and amplitude are greater  
287 compared to other types, which may explain their greater relative influence. Given this, there  
288 is no suggestive evidence for substantial variation in the general shape of the skull among the  
289 species. This pattern is consistent with the strong conservatism in skull traits observed among  
290 small species of Old-World deer, which is thought to be caused by eco-physiological  
291 constraints (Croitor, 2024).

292 It is important to highlight that the sample size of individuals with confirmed sex  
293 identification was not large enough for comparative analysis, making sex a confounding  
294 factor in our results, as males tend to be larger than females (González et al., 2018; Merino et  
295 al., 2005). Even though uncertainty regarding sex classes is included in our results, it did not  
296 seem to significantly affect the overall outcome of four well-distinct groups/species projected  
297 by the linear discriminant functions. A focused analysis with only sexed individuals could  
298 potentially increase predictive power for classifying brocket deer.

299 On the other hand, addressing concerns about multicollinearity, our attempts to reduce its  
300 effects, including the application of Shrinkage Discriminant Analysis (SDA), did not lead to  
301 significant improvements in classification rates. The accuracy of the SDA was comparable to  
302 that of the full LDA model. As an additional approach, we explored a three-dimensional plot  
303 of the first three principal components (PCA) to visualize potential effects of  
304 multicollinearity. However, the PCA failed to correctly group the species as effectively as the  
305 LDA (Suppl. Fig. 2). These findings suggest that collinearity, while present, did not  
306 substantially undermine classification accuracy. This aligns with the understanding that  
307 concerns around variance inflation are more critical for regression models than for  
308 classification purposes.

309 Furthermore, reducing multicollinearity in craniometric studies is challenging due to the  
310 inherent relationships among numerous skull measurements (see Von den Driesch, 1976). In  
311 contexts with limited sample sizes, as in our study, removing correlated variables could  
312 actually reduce classification accuracy. The inclusion of all variables in the full model helped  
313 to mitigate bias, potentially minimized issues like missing data or measurement errors, and  
314 ultimately improved the reproducibility of the results. Thus, the primary goal of maximizing  
315 classification accuracy justified the inclusion of all variables, even in the presence of  
316 collinearity.

317 Finally, although our approach could increase the risk of overfitting, two different model  
318 simplification methods were tested, yielding consistent overall results across different  
319 variable selections. Additionally, despite using <9% imputed data, analyses with different  
320 seeds and randomizations produced consistent classification rates, reinforcing the robustness  
321 of the findings. While the classification rate was generally high, the influence of individual  
322 skull traits on the results must be interpreted with caution, given the intrinsic correlation  
323 among variables.

#### 324 *Evolutionary pathways for inter- and intraspecific craniometric variation*

325 The multidimensional differences in skull size among brocket deer species align with  
326 variations in their average body size (Azevedo et al., 2021). However, whether and to what  
327 extent the evolutionary process of speciation of brocket deer has been directly influenced by



329 variation in body size and the latitudinally variable environmental conditions remains  
330 unclear.

331 From a broad-scale and historical perspective, the latitudinal effect appears to be another  
332 significant factor in body and skull size, especially for wide-ranging deer species. The  
333 Bergmann's rule (increase of body size related to increase in latitude) is commonly observed  
334 and proposed as an adaptive process for many mammals and other endothermic species at  
335 intra- and interspecific levels, as a response towards the optimization of the trade-off between  
336 the body surface (area/volume) and its temperature regulation (Pincheira-Donoso, 2010;  
337 Diniz-Filho et al., 2007; Gilbert et al., 2006; Ashton et al., 2000; Mayr, 1956). While a strong  
338 correlation between size and latitude was found in examinations of a few cervid species  
339 (Clauss et al., 2013), results at the family level may not corroborate Bergmann's or Allen's  
340 rules (Gohli and Voje, 2016).

341 We demonstrated that the skull size of *S. gouazoubira* is partially determined by latitudinal  
342 position, which could influence between 5–53% of the variance in some of the skull  
343 measurements. This intraspecific variation may represent up to 30% of the actual size (e.g.,  
344 BAF – Fig. 5) and supports predictions of Bergmann's rule (Gilbert et al., 2006; Ashton et al.,  
345 2000; Mayr, 1956). Moreover, such a significant allometric pattern emphasizes that skull  
346 size, as a proxy for full body size, is an important morphological trait under natural selection  
347 among brocket deer (Smith et al., 1986).

348 Refined hypotheses for explaining the natural causes of latitudinal variation in body size  
349 among closely related species consider the optimal combination of resource availability and  
350 seasonal environmental constraints determining optimal body size, regulated by energy costs  
351 in each region (Mariño et al., 2023; Rubalcaba et al., 2022). Indeed, at the interspecific level,  
352 recent studies have also provided supplementary controversial information in this context.  
353 For instance, the largest of the gray brocket deer species, which was recently validated  
354 (Sandoval et al., 2024), inhabits tropical areas at the lowest latitudes of South America. On  
355 the other hand, the smallest species among South American cervids are distributed in  
356 temperate to subtropical latitudes (i.e., *Pudu* spp., *Pudella carlae*, and *M. nana* – see Barrio et  
357 al., 2024; Peres et al., 2021a). While Bergmann's rule and other hypotheses on optimization  
358 are originally related to interspecific comparisons, we found that the smallest individuals of  
359 *S. gouazoubira* were at the lowest latitudes, which could be explained by thermoregulation  
360 needs (He et al., 2023). Thus, it appears that the latitudinal influence on deer evolutionary  
361 processes must be primarily taken into consideration as a species-specific process.

362 In this context, the clearly distinct multidimensional size classes among brocket deer  
363 craniometrics led us to suggest that their speciation might have been largely driven by  
364 adaptive processes related to body size variation, a common process among mammals (Baker  
365 et al., 2015; Cooper and Purvis, 2010). While body size is an important trait as a secondary  
366 sexual characteristic favouring larger individuals, we hypothesize that body size may have  
367 favoured disruptive selection rather than a unidirectional process. Although larger male  
368 individuals are more likely to successfully breed in deer polygamous mating systems  
369 (Newbolt et al., 2017), smaller individuals benefit from lower energy requirements and  
370 enhanced mobility in dense forest environments, the primary habitat structure of these  
371 species, thus optimizing their potential niche (Gilbert et al., 2006). As a result, while  
372 selection pressures might also favour smaller individuals due to these ecological advantages,  
373 a trend towards uniformity in cranial patterns may reflect similar eco-physiological  
374 constraints, as observed among Old-World deer (Croitor, 2024).

376 The generalist herbivory of brocket deer denotes strong niche conservatism, which may also  
377 explain the absence of adaptive differences in skull and body shape among species, while  
378 competition for food may likely exerted the main selective pressure, especially during  
379 unfavourable climatic conditions (Olalla-Tárraga et al., 2017). Typical climatic seasonality  
380 and instability in high latitude and elevation regions may facilitate the speciation of distinct  
381 size-classes of closely related species due to more intense adaptive processes (Morales-  
382 Barbero et al., 2021; Diniz-Filho et al., 2007), which may occur independently of phylogeny  
383 (Diniz-Filho et al., 2009). Thus, the speciation process among brocket deer might have been  
384 mainly driven by disruptive selection of body size, likely also due to food competition and as  
385 a result of the occupation of similar forest environments (Duarte et al., 2008). Such  
386 conditions, combined with the occurrence of chromosomal polymorphism, would favour  
387 speciation due to the unlikely potential fertility among distinct size-class and polymorphic  
388 populations of brocket deer (Galindo et al., 2021).

389 Additionally, the combination of slightly overlapped distributions in skull traits of *S.*  
390 *gouazoubira* with *Mazama* spp. suggests that this species might have undergone an early  
391 niche displacement due to interspecific competition with sympatric *Mazama* species before  
392 size-class disruption occurred (Ferreguetti et al., 2015). This hypothesis is supported by the  
393 fact that *S. gouazoubira* is the most habitat generalist among brocket deer species, and  
394 therefore was likely displaced from tropical and subtropical forests to forest edges, riparian  
395 and dry forests, savannahs, and even grassland-like habitats (González et al., 2020; Gallina-  
396 Tessaro et al., 2019). There is also known evidence of differences in daytime activity: the  
397 Gray brocket is mainly diurnal, while *Mazama* species are nocturnal (Srbek-Araujo et al.,  
398 2019). Temporal differentiation was also correlated with differences in habitat use and  
399 occupancy probability between *M. americana* and *S. gouazoubira* (Grotta-Neto, 2020;  
400 Ferreguetti et al., 2015; Rivero et al., 2005), which suggests daytime partitioning as another  
401 component of their ecological niche that would favour species coexistence (Grotta-Neto,  
402 2020; Lucherini et al., 2009; Kronfeld-Schor et al., 2001).

403 Such differences in the realised niche and our results on latitudinal variation in skull size  
404 suggest that the relative influence of body size on the adaptive process of the Gray brocket  
405 may have eased while intraspecific selection increased as the species spatially expanded  
406 throughout its potential adaptive niche throughout the speciation process. This hypothesis  
407 aligns with the consistent estimates of earlier phylogenetic differentiation of the species from  
408 *Mazama* among brocket deer, which are not a monophyletic group (Barrio et al., 2024;  
409 Sandoval et al., 2024; Duarte et al., 2008; Gilbert et al., 2006).

## 410 Conclusion

411 We have assembled the most comprehensive dataset on the craniometrics of sympatric  
412 brocket deer species, combining both published and original data. This foundational dataset is  
413 crucial for future research aimed at refining classification models for brocket deer based on  
414 skull morphology. While the phylogenetic relationships within these groups remain under  
415 investigation, our study supports the use of linear discriminant functions applied to  
416 craniometric data as a statistical tool for validating the taxonomic classification of brocket  
417 deer. We observed that species classification is primarily driven by overall skull size rather  
418 than specific sub-part variation, although factors such as sex and latitude may introduce some  
419 bias. Our findings suggest that the distinct multidimensional variation in skulls among  
420 brocket deer species has likely arisen from disruptive selection on body size. Furthermore, we  
421 provide additional evidence to refine hypotheses regarding the evolutionary history of

brocket deer species. Our results also highlight the importance of maintaining and leveraging biological collections and exploring cost-effective methods (Cook and Light, 2021; Trail, 2021; Ferguson, 2020).

### Acknowledgements

We thank Aline Mantellatto for kindly providing a contextualization and additional details on the molecular identification of brocket deer, especially those from the MHNCI collection. This study received institutional and/or complementary financial support from: Municipal Environmental Secretariat (SMMA) of Curitiba and the Municipal Institute of Public Administration of Curitiba (IMAP), Fundação de Amparo à Pesquisa do Estado de São Paulo (FAPESP), Conselho Nacional de Desenvolvimento Científico e Tecnológico (CNPq), Comisión Sectorial de Investigación Científica de Universidad de la República (CSIC-UDELAR), Programa de Desarrollo de Ciencias Básicas (PEDECIBA), Agencia Nacional de Investigación e Innovación (ANII), and Lóreal-Unesco from Uruguay.

### References

- Abril V.V., Vogliotti A., Varela D.M., Duarte J.M.B., Cartes J.L., 2010. Brazilian dwarf brocket deer *Mazama nana* (Hensel 1872). In: Duarte, J.M.B., González, S (Eds.) Neotropical cervidology: neotropical cervidology biology and medicine of Latin American deer. Funep, Jaboticabal, IUCN, Gland. 160-165.
- Ahdesmaki M., Zuber V., Gibb S., Strimmer K., 2021. sda: Shrinkage Discriminant Analysis and CAT Score Variable Selection. R package version 1.3.8.
- Ashton K., 2004. Sensitivity of intraspecific latitudinal clines of body size for tetrapods to sampling, latitude, and body size. *Integr. Comp. Biol.* 44(5): 403-412.
- Ashton K.G., Tracy M.C., De Queiroz A., 2000. Is Bergmann's rule valid for mammals? *Am. Nat.* 156(4): 390-415.
- Azevedo N.A., Oliveira M.L., Duarte J.M.B., 2021. Guia ilustrado dos cervídeos brasileiros. Sociedade Brasileira de Mastozoologia. Rio de Janeiro.
- Baker J., Meade A., Pagel M., Venditti C., 2015. Adaptive evolution toward larger size in mammals. *PNAS.* 112(16): 5093-5098.
- Barrio J., Gutiérrez E.E., D'Elía G., 2024. The first living cervid species described in the 21st century and revalidation of *Pudella* (Artiodactyla). *J. Mamm.* 105: 577-588.
- Bernegossi A.M., Borges C.H.S., Sandoval E.D.P., Cartes J.L., Cernohorska H., Kubickova S., Vozdova M., Caparroz R., González S., Duarte J.M.B., 2023. Resurrection of the genus *Subulo* Smith, 1827 for the Gray brocket deer, with designation of a neotype. *J. Mamm.* 104: 619-633.
- Borges C.H.S., 2017. Caracterização morfológica, citogenética e molecular de *Mazama gouazoubira* (Artiodactyla, Cervidae) a partir de um topótipo atual. M.Sc. thesis, Faculdade de Ciências Agrárias e Veterinárias, Universidade estadual Paulista "Júlio de Mesquita Filho" Jaboticabal, SP.
- Clauss M., Dittmann M.T., Müller D. W., Meloro C., Codron D., Schulz E., 2013. Bergmann's rule in mammals: A cross-species interspecific pattern. *Oikos.* 122(10): 1465-1472.

463 Cook J.A., Light J.E., 2019. The emerging role of mammal collections in 21st century  
464 mammalogy. *J. Mamm.* 100(3): 733-750.

465 Cooper N., Purvis A., 2010. Body size evolution in mammals: complexity in tempo and mode.  
466 *Am. Nat.* 175(6): 727-738.

467 Croitor R., 2024. A Craniometric Analysis of the Subfamily Cervinae (Cervidae, Mammalia).  
468 *Foss. Stud.* 2(3): 196-222.

469 Diniz-Filho J.A.F., Bini L.M., Rodriguez M.Á., Olalla-Tárraga M.Á., Cardillo M., Hawkins  
470 B.A., 2007. Seeing the forest for the trees: partitioning ecological and phylogenetic  
471 components of Bergmann's rule in European Carnivora. *Ecography.* 30(4): 598-608.

472 Diniz-Filho J.A.F., Rodríguez M.Á., Bini L.M., Hawkins B.A., 2009. Climate history, human  
473 impacts and global body size of Carnivora (Mammalia: Eutheria) at multiple evolutionary  
474 scales. *J. Biogeogr.* 36(12): 2222-2236.

475 Duarte J.M.B., Vogliotti A., Cartes J.L., Oliveira M.L., 2015. *Mazama nana*. The IUCN Red  
476 List of Threatened Species 2015: e.T29621A22154379. Available from  
477 <https://dx.doi.org/10.2305/IUCN.UK.2015-4.RLTS.T29621A22154379.en>. [02 April 2024].

478 Duarte J.M.B., González S., Maldonado J.E. 2008. The surprising evolutionary history of South  
479 American deer. *Mol. Phylogenet. Evol.* 49(1): 17-22.

480 Ferguson A.W., 2020. On the role of (and threat to) natural history museums in mammal  
481 conservation: an African small mammal perspective. *J. Vertebr. Biol.* 69(2): 20028-1.

482 Ferreguetti Á.C., Tomás W.M., Bergallo H.G. 2015. Density, occupancy, and activity pattern  
483 of two sympatric deer (*Mazama*) in the Atlantic Forest, Brazil. *J. Mamm.* 96(6): 1245-1254.

484 Fox J., Weisberg S., 2019. An R Companion to Applied Regression, Third edition. Sage,  
485 Thousand Oaks, CA.

486 Galindo D.J., Vozdova M., Kubickova S., Cernohorska H., Bernegossi A.M., Kadlcikova D.,  
487 Rubes J., Duarte J.M.B., 2021. Sperm chromosome segregation of rob(4;16) and  
488 rob(4;16)inv(4) in the brown brocket deer (*Mazama gouazoubira*). *Theriogenology.* 168: 33-  
489 40.

490 Gallina-Tessaro S., Pérez-Solano L.A., Reyna-Hurtado R., Escobedo-Morales L.A., 2019.  
491 Brocket deer. In: Gallina-Tessaro, S (Ed.) *Ecology and conservation of tropical ungulates in*  
492 *Latin America*. Springer, Cham, Switzerland. 395-414.

493 Gilbert C., Ropiquet A., Hassanin A., 2006. Mitochondrial and nuclear phylogenies of  
494 Cervidae (Mammalia, Ruminantia): Systematics, morphology, and biogeography. *Mol.*  
495 *Phylogenet. Evol.* 40(1):101-117.

496 Gippoliti S., Aloise G., 2016. Why mammal study collections and vouchers are needed in  
497 Italy. *Mus. Sci.* 10: 177-183.

498 Gohli J., Voje K.L., 2016. An interspecific assessment of Bergmann's rule in 22 mammalian  
499 families. *BMC Evol Biol* 16, 222.

500 González S., Aristimuño M.P., Elizondo C., Bidegaray-Batista L., de Faria Peres P.H., Duarte  
501 J.M.B. 2020. Molecular ecology of the southern Gray brocket deer (*Mazama gouazoubira*  
502 Fischer, 1814). *Conserv. Genet. Mamm.* 65-82.

504 González S., Mantellatto A.M.B., Duarte J.M.B., 2018. Craniometrical differentiation of Gray  
505 brocket deer species from Brazil. *Rev. Mus. Argent. Cienc. Nat. Bernardino Rivadavia Inst.*  
506 *Nac. Invest. Cienc. Nat.* 20(1): 1-12.

507 Grotta-Neto F. 2020. Ecologia de cervídeos florestais simpátricos na Mata Atlântica. PhD  
508 thesis, Universidade federal do Paraná, Setor de Ciências Biológicas, Curitiba, PR.

509 Gutiérrez E.E., Helgen K.M., McDonough M.M., Bauer F., Hawkins M.T.R., Escobedo-  
510 Morales L.A., Patterson B.D., Maldonado J.E., 2017. A gene-tree test of the traditional  
511 taxonomy of American deer: the importance of voucher specimens, geographic data, and dense  
512 sampling. *ZooKeys* 697: 87-131.

513 He J., Tu J., Yu J., Jiang H., 2023. A global assessment of Bergmann's rule in mammals and  
514 birds. *Global Change Biol.* 29(18): 5199-5210.

515 Heckeberg N. S., 2020. The systematics of the Cervidae: a total evidence approach. *PeerJ* 8:  
516 e8114.

517 Hua Y., Wang J., Wang H., Zhang W., Vitekere K., Jiang G., 2020. What determines the  
518 success of the species identification? The identification of 10 deer (Cervidae) species in China  
519 based on multiple parameters of hair morphology. *Wildl. Biol.* 2020(3): e00673.

520 IUCN. 2024. The IUCN Red List of Threatened Species. Version 2024-1.  
521 <https://www.iucnredlist.org>. Accessed on [24 September 2024].

522 James, G., Witten, D., Hastie, T., & Tibshirani, R. 2013. *An Introduction to Statistical*  
523 *Learning: With Applications in R*. Springer, New York.

524 Korkmaz S., Goksuluk D., Zararsiz G., 2014. MVN: An R Package for Assessing Multivariate  
525 Normality. *The R Journal.* 6(2): 151-162

526 Kronfeld-Schor N., Dayan T., Elvert R., Haim A., Zisapel N., Heldmaier G. 2001. On the use  
527 of the time axis for ecological separation: diel rhythms as an evolutionary constraint. *Am. Nat.*  
528 158(4): 451-457.

529 Li R., Liu S., Smith K., Che H., 2016. A canonical correlation analysis-based method for  
530 contamination event detection in water sources. *Environ. Sci. Processes Impacts.* 18(6): 658-  
531 666.

532 Lucherini M., Reppucci J.I., Walker R.S., Villalba M.L., Wurstten A., Gallardo G., Iriarte A.,  
533 Villalobos R., Perovic, P. 2009. Activity pattern segregation of carnivores in the high Andes.  
534 *J. Mamm.* 90(6): 1404-1409.

535 Maas C.J., Hox J.J., 2005. Sufficient sample sizes for multilevel modeling. *Methodology.* 1(3):  
536 86-92.

537 Machado F.A., Teta P., 2020. Morphometric analysis of skull shape reveals unprecedented  
538 diversity of African Canidae. *J. Mamm.* 101(2): 349-360.

539 Mahmoudi A., Kryštufek B., Darvish J., Aliabadian M., Yazdi F.T., Moghaddam F.Y.,  
540 Janžekovič F., 2017. Craniometrics are not outdated: Interspecific morphological divergence  
541 in cryptic arvicoline rodents from Iran. *Zool. Anz.* 270: 9-18.

542 Mantellatto A.M.B., González S., Duarte J.M.B., 2020. Molecular identification of *Mazama*  
543 species (Cervidae: Artiodactyla) from natural history collections. *Genet. Mol. Biol.* 43(2):  
544 e20190008.

546 Mantellatto A.M.B., González S., Duarte J.M.B., 2022. Cytochrome b sequence of the *Mazama*  
547 *americana jucunda* Thomas, 1913 holotype reveals *Mazama bororo* Duarte, 1996 as its junior  
548 synonym. Genet. Mol. Biol. 45(1): e20210093.

549 Mariño J., Dufour S.C., Hurford A., Récapet C., 2023. Resource and seasonality drive  
550 interspecific variability in simulations from a dynamic energy budget model. Conserv. Physiol.  
551 11(1): coad013.

552 Mayr E., 1956. Geographical character gradients and climatic adaptation. Evolution. 10:105-  
553 108.

554 McNab B.K., 2010. Geographic and temporal correlations of mammalian size reconsidered: a  
555 resource rule. Oecologia. 164(1): 13-23.

556 Mera-Gaona M., Neumann U., Vargas-Cañas R., López D.M., 2021. Evaluating the impact of  
557 multivariate imputation by MICE in feature selection. PLoS ONE. 16(7): e0254720.

558 Merino M.L., Milne N., Vizcaíno S.F., 2005. A cranial morphometric study of deer  
559 (Mammalia, Cervidae) from Argentina using three-dimensional landmarks. Acta Theriologica.  
560 50(1): 91-108.

561 Morales-Barbero J., Gouveia S.F., Martinez P.A., 2021. Historical climatic instability predicts  
562 the inverse latitudinal pattern in speciation rate of modern mammalian biota. J. Evol. Biol.  
563 34(2): 339-351.

564 Morales-Donoso J.A., Vacari G.Q., Bernegossi A.M., Sandoval E.D.P., Peres P.H.F., Galindo  
565 D.J., de Thoisy B., Vozdova M., Kubickova S., Duarte J.M.B., 2023. Revalidation of *Passalites*  
566 Gloger, 1841 for the Amazon brown brocket deer *P. nemorivagus* (Cuvier, 1817) (Mammalia,  
567 Artiodactyla, Cervidae). ZooKeys. 1167: 241-264.

568 Munkhzul T., Reading R.P., Buuveibaatar B., Murdoch J.D., 2018. Comparative craniometric  
569 measurements of two sympatric species of *Vulpes* in Ikh Nart Nature Reserve,  
570 Mongolia. Mong. J. Biol. Sci. 16(1): 19-28.

571 Newbolt C.H., Acker P.K., Neuman T.J., Hoffman S.I., Ditchkoff S.S., Steury T.D. 2017.  
572 Factors influencing reproductive success in male white-tailed deer. J. Wildl. Manage. 81(2):  
573 206-217.

574 Olalla-Tárraga M.Á., González-Suárez M., Bernardo-Madrid R., Revilla E., Villalobos F.  
575 2017. Contrasting evidence of phylogenetic trophic niche conservatism in mammals  
576 worldwide. J Biogeography. 44(1): 99-110.

577 Oliveira M.L., Grotta-Netto F., Peres P.H.F., Vogliotti A., Brocardo C.R., Cherem J.J., Landis  
578 M., Faolino R.M., Fusco-Costa R., Gatti A., Moreira D.O., Ferreira P.M., Mendes S.L.,  
579 Huguenin J., Zanin M., Nodari J.Z., Leite Y.L.R., Lyrio G.S., Ferraz K.M.P.M.B., Passos F.C.,  
580 Duarte J.M.B., 2022. Elusive deer occurrences at the Atlantic Forest: 20 years of surveys.  
581 Mamm Research. 67: 51-59.

582 Peres P.H.F., Grotta-Netto F., Luduvério D.J., Oliveira M.L., Duarte J.M.B., 2021b.  
583 Implications of unreliable species identification methods for Neotropical deer conservation  
584 planning. Perspect. Ecol.Conser. 19(4): 435-442.

585 Peres P.H.F., Luduvério D.J., Bernegossi A.M., Galindo D.J., Nascimento G.B., Oliveira M.L.,  
586 Sandoval E.D.P., Vozdova M., Kubickova S., Cernohorska H., Duarte J.M.B., 2021a.  
587 Revalidation of *Mazama rufa* (Illiger 1815) (Artiodactyla: Cervidae) as a Distinct Species out  
588 of the Complex *Mazama americana* (Erxleben 1777). Front Genet. 12:742870.

590 Pincheira-Donoso D., 2010. The balance between predictions and evidence and the search for  
591 universal macroecological patterns: taking Bergmann's rule back to its endothermic origin.  
592 Theory Biosci. 129(4): 247-253.

593 Pires A.C., Marinoni L., 2010. DNA barcoding and traditional taxonomy unified through  
594 Integrative Taxonomy: a view that challenges the debate questioning both methodologies.  
595 Biota Neotrop. 10(2): 339-346.

596 R Core Team, 2024. R: A language and environment for statistical computing. R Foundation  
597 for Statistical Computing, Vienna, Austria. <https://www.R-project.org/>.

598 Rivero K., Rumiz D.I., Taber A.B. 2005. Differential habitat use by two sympatric brocket deer  
599 species (*Mazama americana* and *M. gouazoubira*) in a seasonal Chiquitano forest of Bolivia.  
600 Mammalia. 69(2): 169-183.

601 Rossi R.V., 2000. Taxonomia de *Mazama rafinesque*, 1817 do Brasil (Artiodactyla, Cervidae).  
602 PhD thesis, Instituto de Biociências, Universidade de São Paulo, São Paulo, SP.

603 Rubalcaba J.G., Gouveia S.F., Villalobos F., Olalla-Tárraga M.Á., 2022. Physical constraints  
604 on thermoregulation and flight drive morphological evolution in bats. Proc. Natl. Acad. Sci.  
605 119(15): e2103745119.

606 Sandoval E.D.P., Jędrzejewski W., Molinari J., Vozdova M., Cernohorska H., Kubickova S.,  
607 Bernegossi A.M., Caparroz R., Duarte J.M.B., 2024. Description of *Bisbalus*, a New Genus for  
608 the Gray Brocket, *Mazama* cita Osgood, 1912 (Mammalia, Cervidae), as a Step to Solve the  
609 Neotropical Deer Puzzle. Taxonomy. 4: 10-26.

610 Sandoval E.D.P., Vacari G.Q., Juliá J.P., González S., Vozdova M., Cernohorska H.,  
611 Kubickova S., Kalthoff D.C., Duarte J.M.B., 2023. Assessing the Taxonomic Status of the  
612 Gray Brocket *Mazama simplicicornis* argentina Lönnberg, 1919 (Artiodactyla: Cervidae).  
613 Zool. Stud. 62: e30.

614 Sievert C., 2020. Interactive Web-Based Data Visualization with R, plotly, and shiny.  
615 Chapman and Hall/CRC Florida.

616 Silva B.F.S., Oliveira M.L., Duarte J.M.B., 2020. Assessing the morphological identification  
617 of guard hairs from Brazilian deer. Iheringia, Ser. Zool. 110: e2020029.

618 Smith M.H., Branam W.V., Marchinton R.L., Johns P.E., Wooten M.C., 1986. Genetic and  
619 morphologic comparisons of Red brocket, Brown brocket, and White-tailed deer. J. Mamm.  
620 67(1): 103-111.

621 Suchentrunk F., Flux J.E.C., Flux M.M., Slimen H.B., 2007. Multivariate discrimination  
622 between East African cape hares (*Lepus capensis*) and savanna hares (*L. victoriae*) based on  
623 occipital bone shape. Mamm. Biol. 72(6): 372-383.

624 Srbeć-Araújo A.C., Cecanecchia G.C., Cecanecchia G.C., 2019. Activity Pattern of Brocket  
625 Deer (Genus *Mazama*) in the Atlantic Forest. JOJ Wild. Biod. 1(2): 63-71.

626 Tamagnini D., Canestrelli D., Meloro C., Raia P., Maiorano L., 2021. New Avenues for Old  
627 Travellers: Phenotypic Evolutionary Trends Meet Morphodynamics, and Both Enter the Global  
628 Change Biology Era. Evol. Biol. 48: 379–393.

629 Thier N., Ansoorge H., Stefen C., 2020. Assessing geographic differences in skulls of *Neomys*  
630 *fodiens* and *Neomys anomalus* using linear measurements, geometric morphometrics, and non-  
631 metric epigenetics. Mamm. Res. 65: 19-32.

633 Trail P.W., 2021. Morphological analysis: A powerful tool in wildlife forensic  
634 biology. *Forensic Sci. Int. Anim. Environ.* 1: 100025.

635 Van Buuren S., Groothuis-Oudshoorn K. 2011., MICE: Multivariate Imputation by Chained  
636 Equations in R. *J. Stat. Software.* 45(3): 1-67.

637 Venables W.N., Ripley B.D., 2002. *Modern Applied Statistics with S.* Stat. Comput. Fourth  
638 Edition.

639 Vogliotti A., Oliveira M.L., Duarte J.M.B., 2016. *Mazama bororo*. The IUCN Red List of  
640 Threatened Species 2016: e.T41023A22155086. Available from  
641 <https://dx.doi.org/10.2305/IUCN.UK.2016-1.RLTS.T41023A22155086.en>. [02 April 2024].

642 Von den Driesch A., 1976. A guide to the measurement of animal bones from archaeological  
643 sites. Peabody Museum Bulletin 1. Peabody Museum of Archaeology and Ethnology. Harvard  
644 University, Cambridge.

645 Weihs C., Ligges U., Luebke K., Raabe N., 2005. klaR Analyzing German Business Cycles.  
646 In: Gaul, W., Vichi, M., Weihs, C (Eds.) *Studies in Classification, Data Analysis, and*  
647 *Knowledge Organization.* Springer. 335-343.



Table 1. Craniometric data source and sample size for five brocket deer species included in this study.

Source	Species				
	<i>M. americana</i>	<i>M. jucunda</i>	<i>M. nana</i>	<i>M. rufa</i>	<i>S. gouazoubira</i>
Borges 2017, Bernegossi et al. 2022	-	-	-	-	1
González et al. 2018	-	1	-	-	8
MHNCI (Mantellatto et al. 2020)	2	8	7	-	8
MHNCI	5	2	1	-	3
Peres et al. 2021a	11	4	4	4	-
Sandoval et al. 2023	1	-	-	-	10
Total	19	15	12	4	30

Table 2. Confusion matrix of observations vs. full model predictions.

Group/species	<i>americana</i>	<i>gouazoubira</i>	<i>jucunda</i>	<i>nana</i>
<i>americana</i>	23	0	0	0
<i>gouazoubira</i>	0	29	1	0
<i>jucunda</i>	0	0	14	0
<i>nana</i>	0	1	0	12

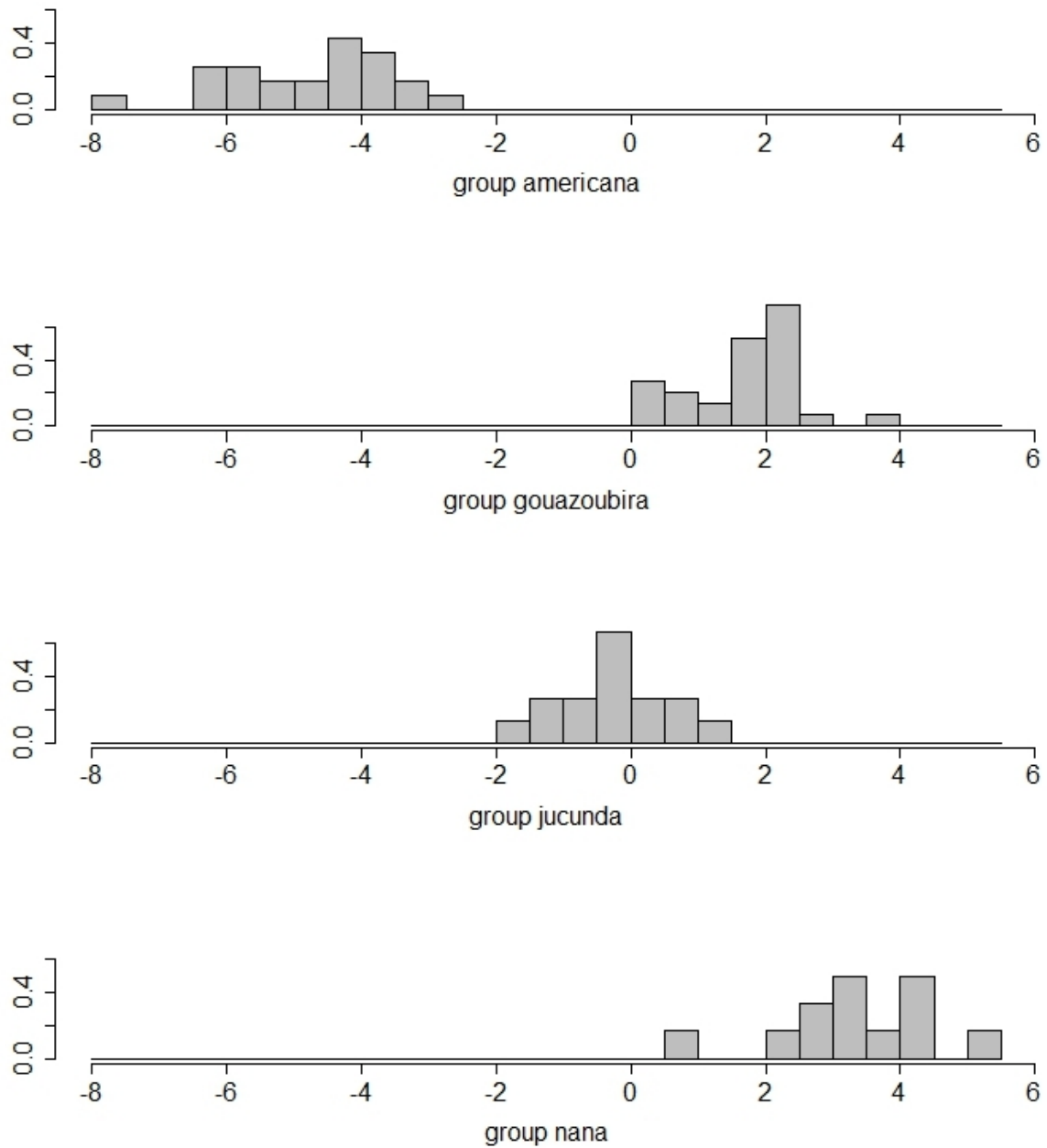
Table 3. The ten most important morphological traits of brocket deer skull for group classification by linear discriminant functions based on the explained variance of each variable.

<u>LD1</u>		<u>LD2</u>		<u>LD3</u>	
Trait	Variance (%)	Trait	Variance (%)	Trait	Variance (%)
SSL	32	BL	11	LR	26
LR	10	LT	8	ZYB	11
MFL	8	GBBC	8	LCHEE	9
LP	8	LN	8	BAF	8
PREPRO	8	GHOR	8	BL	6
GHOR	4	MFL	8	GBBC	5
GLOR	4	GBOC	7	LBBO	4
BAF	4	GBOC	7	LP	4
LN	3	GBAO	6	GBFM	4
LCHEE	3	ACI	5	LFBO	3
		LLPRMAX	5		

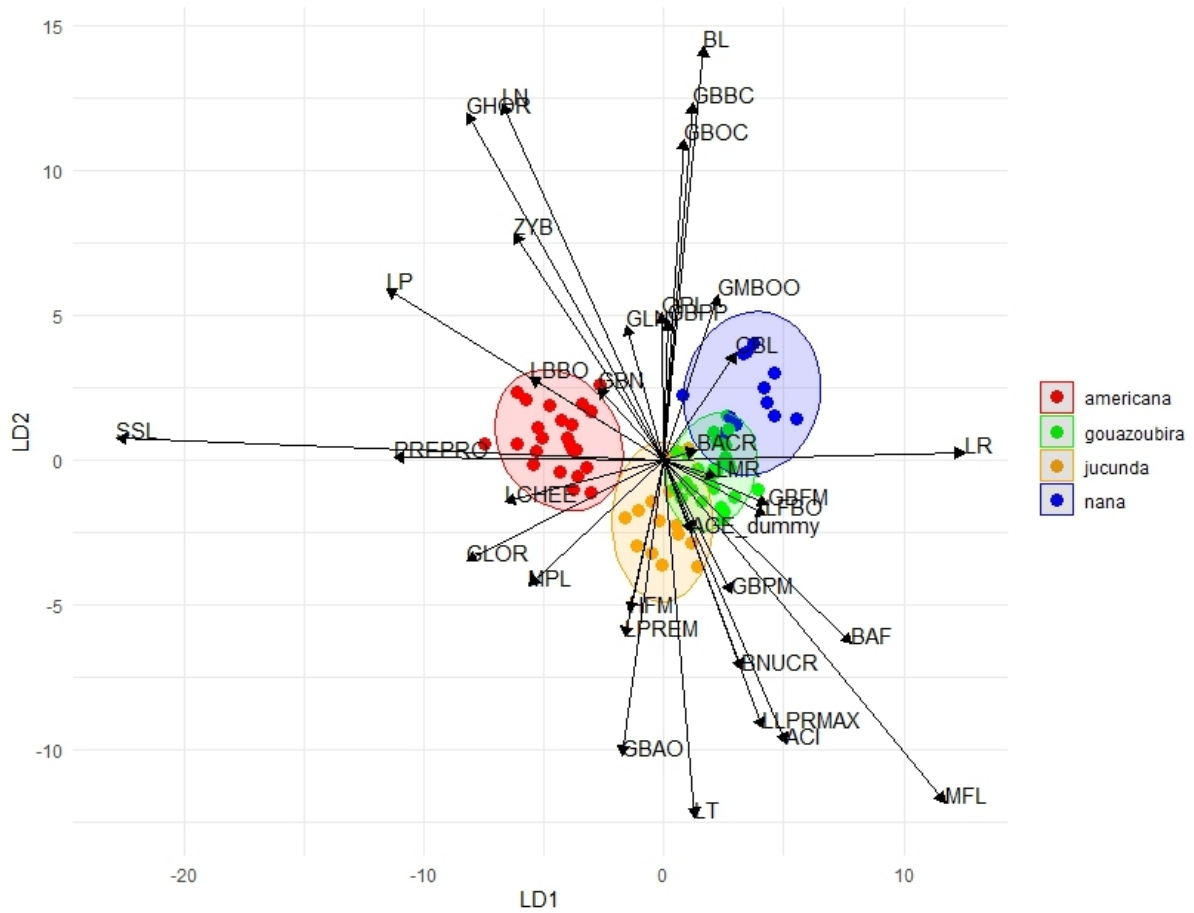


Table 4. Sample size, coefficient of determination and significance of linear regressions tests for selected skull variables of the four sympatric groups/species of brocket deer.

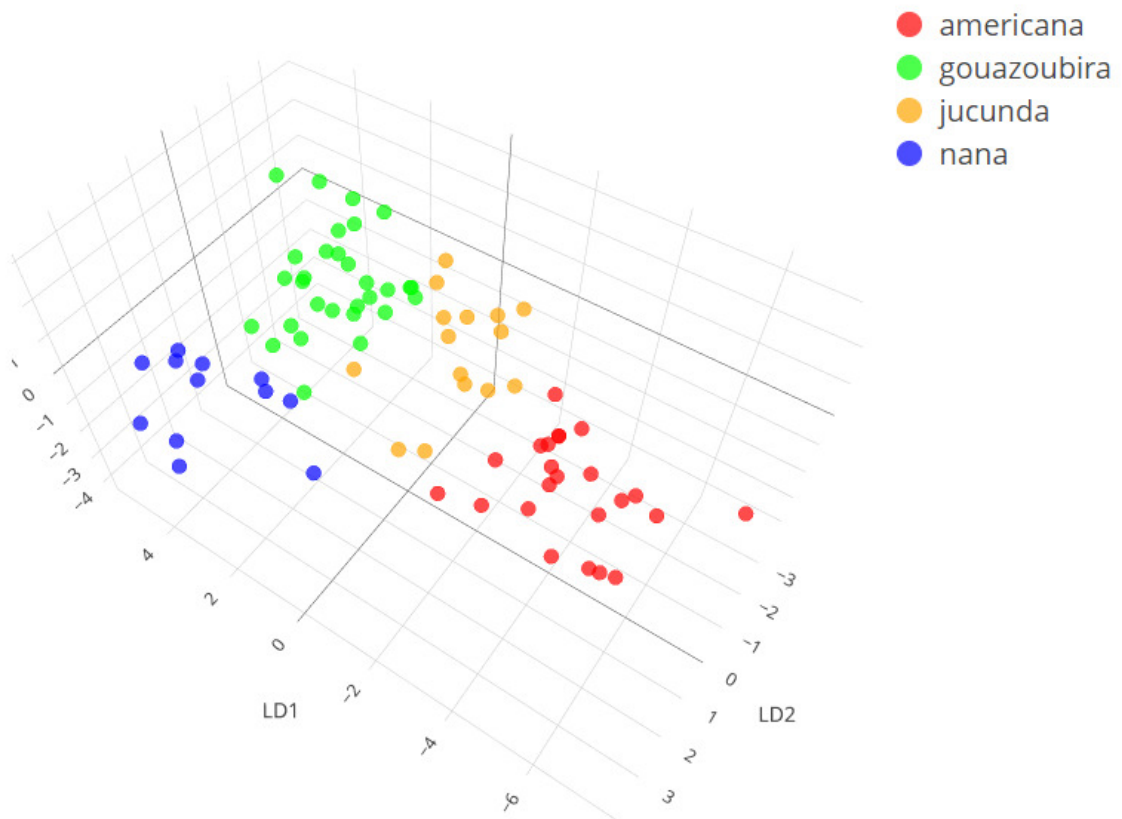
Variable	n	R <sup>2</sup>	p	Signif.
BAF	47	0,53	<0.001	***
LR	50	0,26	<0.001	***
LT	58	0,22	<0.01	**
LP	49	0,19	<0.01	**
CBL	57	0,16	<0.01	**
BL	56	0,15	<0.01	**
LLPRMAX	59	0,12	<0.01	**
MFL	53	0,12	<0.05	*
ZYB	60	0,07	<0.05	*
LCHEE	62	0,04	>0.05	-
LPREM	62	0,03	>0.05	-
SSL	59	0	>0.05	-



Distribution of projections of observations onto the first axis of linear discriminant analysis for the four sympatric groups/species of brocket deer.

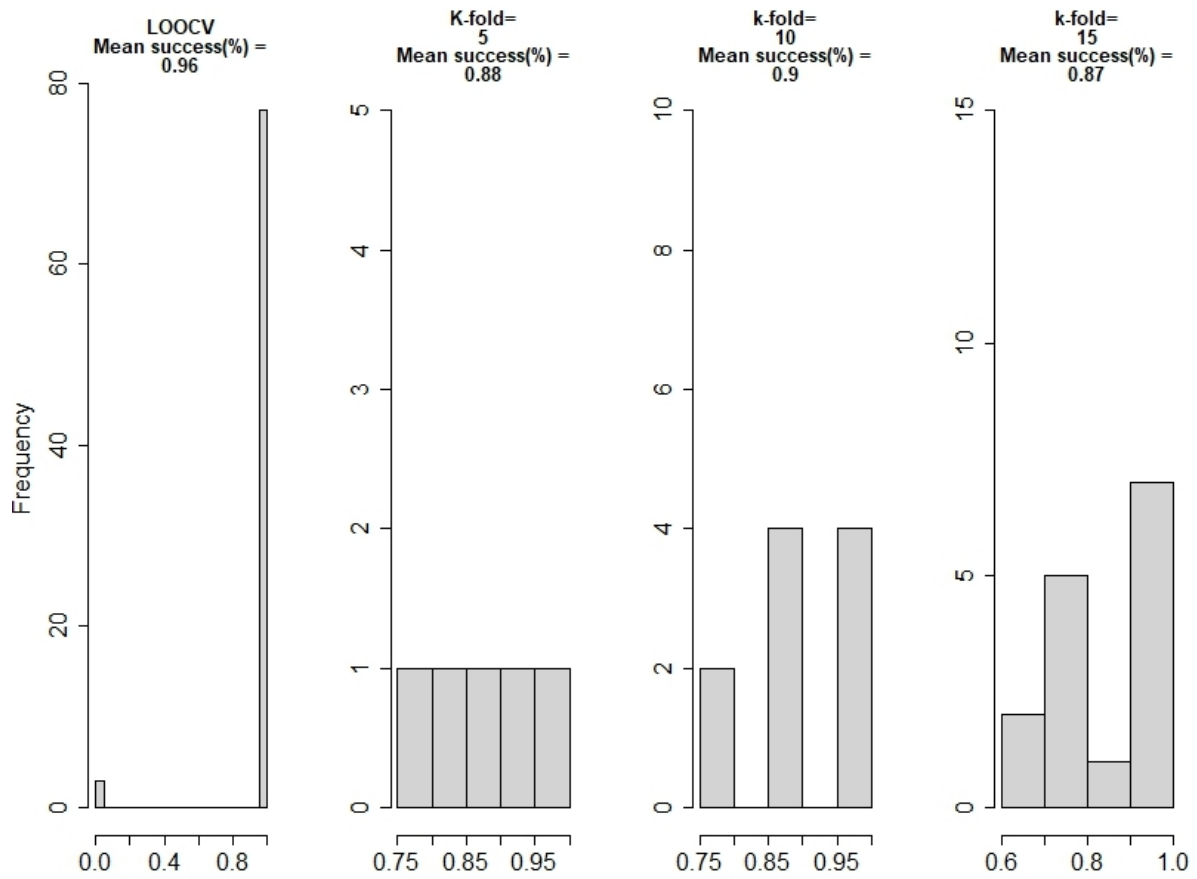


Two-dimensional scatterplot of projections of observations onto the first two axes of the linear discriminant analysis (related to 91.7% of total variance) and variables' directions and effect intensity for classifying four sympatric groups/species of brocket deer.

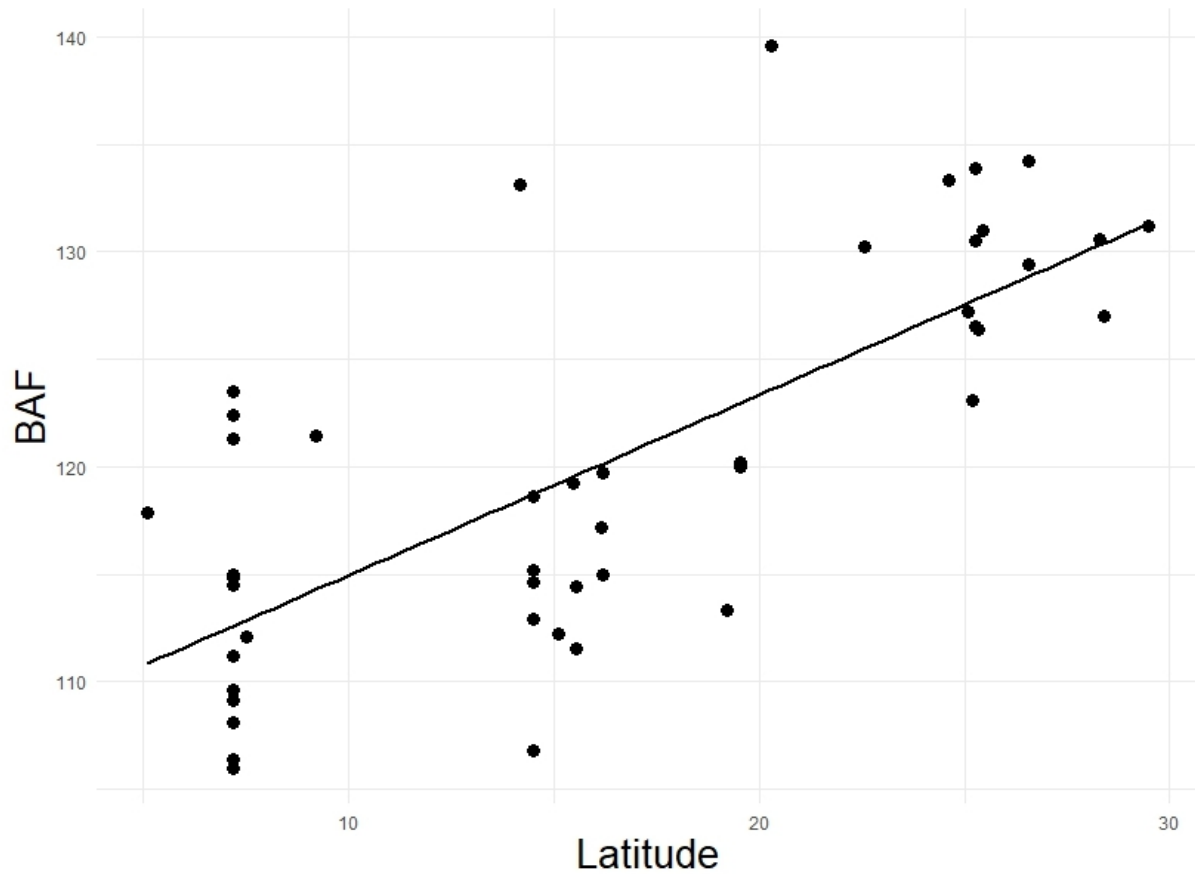


Three-dimensional scatterplot of projections of observations onto the three axes of the linear discriminant analysis considering four sympatric groups/species of brocket deer.





Distribution and mean success of classifications based on four cross-validation procedures: LOOCV and K-fold with K = 5, 10 and 15.



Scatterplot and fitting regression model showing a strong relationship ( $R^2=0.53$ ) between the size of the basifacial axis (BAF) in the skull of Gray brocket deer *Subulo gouazoubira* against latitude of origin in South America.

**Manuscript body**

[Download source file \(51.81 kB\)](#)

**Tables**

Table 1 - [Download source file \(11.2 kB\)](#)

Craniometric data source and sample size for five brocket deer species included in this study.

Table 2 - [Download source file \(10.46 kB\)](#)

Confusion matrix of observations vs. full model predictions.

Table 3 - [Download source file \(11.16 kB\)](#)

The ten most important morphological traits of brocket deer skull for group classification by linear discriminant functions based on the explained variance of each variable

Table 4 - [Download source file \(10.98 kB\)](#)

Sample size, coefficient of determination and significance of linear regressions tests for selected skull variables of the four sympatric groups/species of brocket deer.

**Figures**

Figure 1 - [Download source file \(75.62 kB\)](#)

Distribution of projections of observations onto the first axis of linear discriminant analysis for the four sympatric groups/species of brocket deer.

Figure 2 - [Download source file \(157.11 kB\)](#)

Two-dimensional scatterplot of projections of observations onto the first two axes of the linear discriminant analysis (related to 91.7% of total variance) and variables' directions and effect intensity for classifying four sympatric groups/species of brocket deer.

Figure 3 - [Download source file \(70.14 kB\)](#)

Three-dimensional scatterplot of projections of observations onto the three axes of the linear discriminant analysis considering four sympatric groups/species of brocket deer.

Figure 4 - [Download source file \(94.61 kB\)](#)

Distribution and mean success of classifications based on four cross-validation procedures: LOOCV and K-fold with K = 5, 10 and 15.

Figure 5 - [Download source file \(62.59 kB\)](#)

Scatterplot and fitting regression model showing a strong relationship ( $R^2=0.53$ ) between the size of the basifacial axis (BAF) in the skull of Gray brocket deer *Subulo gouazoubira* against latitude of origin in South America.

**Supplementary Online Material**

File 1 - [Download source file \(121.61 kB\)](#)

Supplementary Tables and Figures.

File 2 - [Download source file \(3.7 MB\)](#)

Supplementary Material 2 - Interactive 3D plot

File 3 - [Download source file \(25.51 kB\)](#)

Dataset

File 4 - [Download source file \(4.85 MB\)](#)

A rotating 3D plot as GIF file.